

Kinetics of oxidation of hydroquinones by molecular oxygen. Effect of superoxide dismutase

2 PERKIN

Vitaly Roginsky* and Tatyana Barsukova

*N. Semenov Institute of Chemical Physics, Russian Academy of Sciences, Kosygin St. 4,
117977 Moscow, Russia*

Received (in Cambridge, UK) 18th January 2000, Accepted 5th April 2000

Published on the Web 1st June 2000

The kinetics of the autoxidation of sixteen hydroquinones (QH₂) (substituted 1,4-hydroquinones and 1,4-dihydroxynaphthalenes as well as 9,10-dihydroxyphenanthrene) were studied using the Clark electrode technique in aqueous solution, pH 7.40, at 37 °C both with and without added superoxide dismutase (SOD). QH₂ oxidation occurs typically with a self-acceleration. A maximum rate of oxidation, R_{MAX} , was found to be the most indicative parameter characterizing QH₂ oxidizability. A kinetic scheme of QH₂ autoxidation was developed; computer simulations carried out on the basis of this scheme reproduce the main kinetic features of the studied process. QH₂ autoxidation is suggested to be a free-radical chain process with semiquinone (Q^{•-}) and superoxide (O₂^{•-}) as chain-carrying species. The oxidation is initiated by reaction (1) $\text{Q} + \text{QH}_2 \rightarrow 2\text{Q}^{\bullet-} + 2\text{H}^+$. The addition of SOD results in two main effects: shifting the equilibrium (2) $\text{Q}^{\bullet-} + \text{O}_2 \rightleftharpoons \text{Q} + \text{O}_2^{\bullet-}$ (K_2) to the right and suppressing reaction (3) $\text{QH}_2 + \text{O}_2^{\bullet-} \rightarrow \text{Q}^{\bullet-} + \text{H}_2\text{O}_2$. The net effect of SOD depends basically on K_2 . When $K_2 < 0.1$, the addition of SOD results in stimulation of the oxidation; when $K_2 > 0.1$, the more SOD inhibits the oxidation, the higher K_2 . The concentration of SOD causing the 50%-effect on R_{MAX} ($[\text{SOD}]_{50}$), both inhibitory and stimulatory, decreases dramatically when K_2 increases. At $[\text{SOD}] \gg [\text{SOD}]_{50}$ the rate of QH₂ autoxidation is definitively determined by the rate of reaction (1). For the majority of QH₂, $[\text{SOD}]_{50}$ is significantly less than the physiological values of [SOD] and thus QH₂ autoxidation in biological environment is expected to occur in the above kinetically simple mode.

Introduction

Hydroquinones (QH₂) are thermodynamically less stable at neutral pH than the corresponding quinones (Q). However, Q can be effectively converted into QH₂ by several one- and two-electron mechanisms,¹⁻³ so QH₂ usually coexist with Q in biological systems. Some QH₂ may also be formed by enzymatic hydroxylation of various aromatic compounds as well as by biosynthesis (mainly *ortho*-hydroquinones), e.g. catecholamines in animals, flavonoids and tannins in plants.

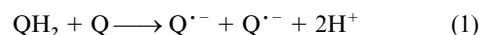
Many QH₂ are highly reactive and thus play a remarkable role in a variety of biologically significant processes. Autoxidation is the most characteristic reaction of QH₂. Although kinetic studies of QH₂ autoxidation have received much attention in the literature,¹⁻¹⁵ the data obtained are often contradictory. In various works, experiments have been performed at different pH, temperatures, and starting concentrations of QH₂; this makes it possible to compare the reactivity of various compounds within a single work only. As a rule, authors report the rate of oxidation determined only at a single concentration of QH₂. Sometimes it is difficult to understand from the text which rate of the process, initial or maximum, has been reported. Under these circumstances, many subtle details of the process remain unnoticed. The recent study on the autoxidation of non-substituted 1,4-hydroquinone⁷ is among uncommon exceptions. In many cases, the oxidation of QH₂ has been studied under conditions of their concomitant formation by the enzymatic^{11,13,16} or chemical^{3,4} reduction of Q. In doing so, the acting concentrations of QH₂ and Q are commonly known with a poor accuracy.

Although the principle products of QH₂ autoxidation, the corresponding Q and H₂O₂, are well known, there is no consensus on the mechanism of the process under consideration. In the majority of works, autoxidation is considered to be triggered by direct interaction of QH₂ with molecular oxygen.

Meantime, reaction (0) is spin-restricted and thus expected to

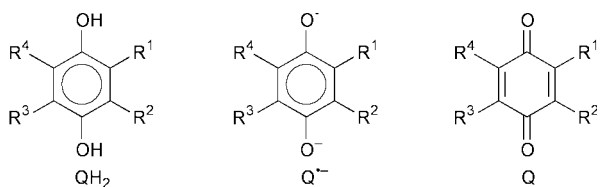


be extremely slow under physiological conditions.^{7,15} Alternatively, the oxidation of QH₂ by molecular oxygen is considered as a catalytic process. Transition metals have been often documented as catalysts of oxidation.¹⁵ However, the presence of transition metals as catalysts is not imperative to the occurrence of the oxidation. Q, being a product of QH₂ oxidation, can serve as a catalyst along with transition metals. This has been evidenced by the fact that autoxidation of many QH₂ occurs with a visible self-acceleration^{5,7,14} and may be also accelerated by adding Q.^{5,7} This suggests that the process is likely triggered by the reaction (1).

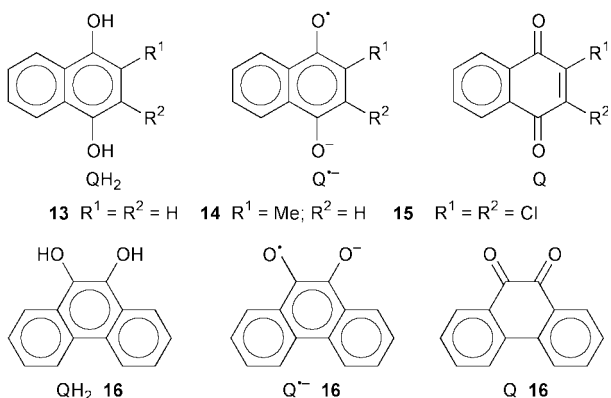


Meanwhile, the main factors determining the oxidizability of QH₂ remain unknown. Repeated attempts have been undertaken to correlate the oxidizability of QH₂ with their one-electron reduction potential $E(\text{Q}^{\bullet-}/\text{QH}_2)$ ^{1,2} and two-electron reduction potential $E(\text{Q}/\text{QH}_2)$.¹⁷ These attempts have had only moderate success and many compounds dropped out of the correlation. This is a reason why some authors^{1,11} have come to the conclusion that QH₂ oxidizability does not correlate with any reduction potential. While it has been repeatedly speculated^{3,7} that the rate of QH₂ autoxidation is controlled by the rate of reaction (1), this idea has not yet been experimentally supported.

In this work, the Clark electrode technique has been used to study in detail the kinetics of oxygen consumption during the autoxidation of sixteen hydroquinones (compounds 1–16); seven of them have been studied for the first time. Special attention has been paid to the effect of superoxide dismutase (SOD), bearing in mind the oxidation of hydroquinones under *in vivo*



	R ¹	R ²	R ³	R ⁴
1	H	H	H	H
2	Me	H	H	H
3	Et	H	H	H
4	Bu ^l	H	H	H
5	Me	H	H	Me
6	Me	Me	H	H
7	Me	H	Me	H
8	Me	Me	Pr ⁱ	H
9	OMe	H	H	OMe
10	OH	H	CH ₂ CH ₂ NH ₂	H
11	Me	Me	Me	H
12	OMe	OMe	OMe	H



conditions. Computer simulations have allowed us to elucidate many kinetic details of this process. In particular, it has been found that the rate of oxidation is basically determined by the rate of reaction (1) and only moderately depends on other factors when the oxidation occurs in the presence of physiological concentrations of SOD.

Experimental

Of the hydroquinones (QH₂) studied in this work **6**, **11** and **13** were purchased from Aldrich; **10** was obtained from Sigma; **3** was a gift from H. B. Stegmann. All the other QH₂ were prepared from the corresponding quinone (Q). Quinones **1**, **5**, **8**, **14** and **16** were purchased from Aldrich; **12** was purchased from Sigma; **2** from Merck; **9** from Lancaster; **7** and **15** were obtained from Fluka; **4** from EGA Chemie. The above Q were converted into QH₂ by reduction with sodium tetrahydroborate in tetrahydrofuran or with Zn powder in acetic acid using the standard procedures. With the exception of compound **10**, both purchased and synthesized QH₂ were purified by recrystallization from an appropriate solvent or using a silica gel (40–100 μm) column with CHCl₃ as an eluent. Superoxide dismutase from bovine erythrocytes with activity of 4000–7000 U mg⁻¹ was purchased from Sigma. Sodium phosphates, NaH₂PO₄ and Na₂HPO₄, of the highest grade, used to prepare buffer solution, were purchased from Merck.

Aqueous solutions were prepared with doubly distilled water. Experiments were performed at 37.0 ± 0.1 °C with 50 mM phosphate buffer, pH 7.40 ± 0.02 (unless otherwise indicated), which was prepared by mixing 50 mM solutions of NaH₂PO₄ and Na₂HPO₄ without adding any acid or base. Solutions of the individual phosphates used for the buffer preparation were purged from traces of transition metals by Chelex-100 resin

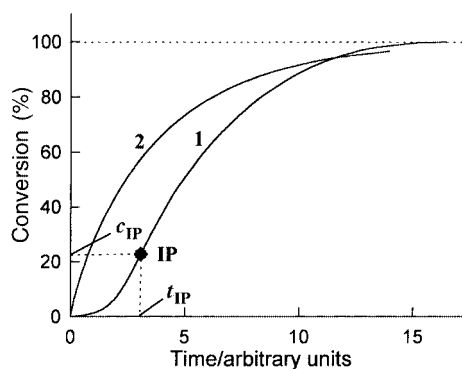


Fig. 1 Types of [O₂] traces observed during the autoxidation of QH₂. Plot 1—an S-shaped trace ((S)-type); symbol ♦ shows the position of the inflection point (IP); *c*_{IP} is a conversion at IP; *t*_{IP} is the time required to reach IP. Plot 2—a trace with a progressively reduced rate of oxygen uptake ((–)-type).

(Bio-Rad) using a batch method. Stock solutions of QH₂ were prepared with acid aqueous methanol under argon atmosphere and stored no longer than one day at –25 °C.

The kinetics of oxygen consumption accompanying QH₂ autoxidation were studied with a 5300 Oxygen Biological Monitor (Yellow Springs Instruments Co., USA) equipped with a Clark electrode as a sensor. Runs were started by adding QH₂ stock solution. The rate of oxygen consumption was calculated from the slope of [O₂] traces. The protocols describing preparation of solutions and kinetic studies of oxygen consumption have been given in more detail in our previous publications.^{5,18–21}

Kinetic computer simulations were performed using the program 'Kinetics' (based on the Gear method) elaborated by A. Sokolov and I. Utkin.

Results and discussion

Shape of [O₂] traces

Most typically, QH₂ autoxidation develops with a pronounced auto-acceleration. The kinetics of oxygen uptake accompanying this process are schematically presented in Fig. 1. Two types of [O₂] traces have been observed. The S-shaped traces (plot 1) are most characteristic of QH₂ oxidation in the presence of SOD. At the early stage, the process develops sometimes so slowly that some authors^{7,12} write about a lag phase. Since the duration of the lag-phase is a somewhat vague value, complicated to determine both experimentally and theoretically, it seems more rational to repudiate of this in favor of the inflection point (IP), when the rate of oxidation reaches a maximum value, *R*_{MAX}. A trace of the S-type may be characterized by *R*_{MAX}, the position of IP, the period of time required to arrive at IP (*t*_{IP}), as well as by conversion at IP (*c*_{IP}) (Fig. 1). The latter varies from zero to the theoretically maximum value of 50% (see below). Sometimes traces of the (–)-type (plot 2) are observed, when the rate of oxidation decreases from the very beginning; in this case *R*_{MAX} coincides with the initial rate. Meanwhile, the theoretical consideration given below shows that there is no fundamental difference between traces of the S- and (–)-type. When we deal with traces of the (–)-type, IP is actually reached so fast and at such low conversion that it cannot be experimentally detected. However, this can always be done by computer simulation. Typically, the mole ratio of the total oxygen consumed to QH₂ oxidized is nearly 1 : 1 (Fig. 2).

The relationship between the kinetics of oxidation and hydroquinone structure

The values of *R*_{MAX} determined during the oxidation of various QH₂ under 'standard' conditions (37 °C, pH 7.4, [QH₂] = 100

Table 1 Effect of SOD on the kinetics of the oxidation of 100 μM hydroquinones in 50 mM phosphate buffer, pH 7.40, at 37 $^{\circ}\text{C}$

QH ₂ ^a	$R_{\text{MAX}}/\text{nM s}^{-1b}$		$(R_{\text{MAX}})_{\text{SOD}}/(R_{\text{MAX}})_0$
	-SOD ($R_{\text{MAX}})_0$	+SOD ($R_{\text{MAX}})_{\text{SOD}}^c$	
1	3 \pm 1 (-)	550 (S) ^d	180
2	12 \pm 2 (-)	250 \pm 15 (S)	20
3	6.5 \pm 1.5 (-)	145 \pm 10 (S)	22
4	2.5 \pm 1 ^e	2.5 \pm 1 ^e	~1
5	10 \pm 2 (-)	46 \pm 4 (S)	4.6
6	12 \pm 2 (S)	45 \pm 4 (S)	3.8
7	15 \pm 2 (S)	60 \pm 4 (S)	4.0
8	6.5 \pm 1.5 (-)	28 \pm 3 (S)	4.3
9	710 \pm 50 (S)	1030 \pm 80 (S)	1.5
10	880 \pm 70 (-)	110 \pm 10 (S)	0.13
11	14.5 \pm 2.0 (S)	22 \pm 2 (S)	1.5
12	55 \pm 4 (S)	140 \pm 10 (S)	2.5
13	3000 \pm 150 (S)	4200 \pm 200 (S)	1.4
14	2500 \pm 120 (S)	1070 \pm 80 (S)	0.43
15	12000 \pm 1000 ^f	>12000 ^f	>1
16	>8600 ^g (-)	>5900 ^g (S)	~0.7

^a Structures of QH₂ are given in the text. ^b Values of R_{MAX} mean \pm SD from three or more independent experiments; (-) and (S) indicate the type of [O₂] traces (see text). ^c Determined at the optimal concentration of SOD (see text). ^d Taken from ref. 7. ^e ($R_{\text{MAX}})_0 = 21 \pm 3 \text{ nM s}^{-1}$ (-) and ($R_{\text{MAX}})_{\text{SOD}} = 67 \pm 5 \text{ nM s}^{-1}$ (S) when determined at pH 8.2. ^f ($R_{\text{MAX}})_0 = 390 \pm 25 \text{ nM s}^{-1}$ (-) and ($R_{\text{MAX}})_{\text{SOD}} = 780 \pm 60 \text{ nM s}^{-1}$ (S) when determined at pH 4.7. ^g Only estimated because of poor stability of stock solution.

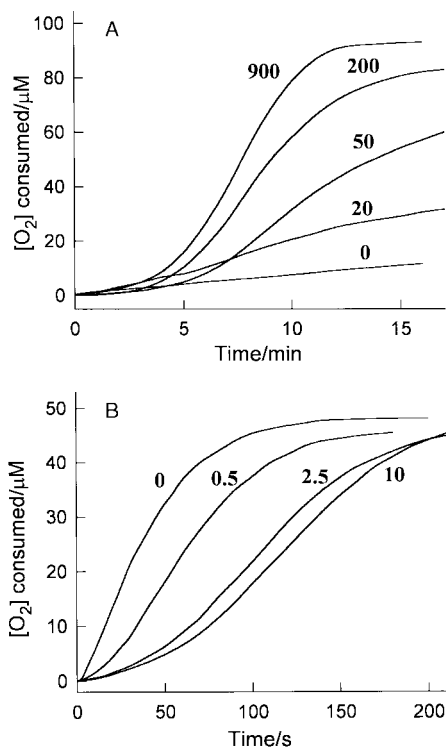


Fig. 2 Effect of SOD on the kinetics of the oxidation of 100 μM QH₂ 2 (A) and 50 μM QH₂ 14 (B) in phosphate buffer, pH 7.40, at 37 $^{\circ}\text{C}$. Figures at traces mean SOD concentration in U ml^{-1} .

μM) are listed in Table 1. Table 1 also reports the type of trace observed and the effect of SOD addition expressed as $(R_{\text{MAX}})_{\text{SOD}}/(R_{\text{MAX}})_0$ where $(R_{\text{MAX}})_0$ is R_{MAX} without SOD and $(R_{\text{MAX}})_{\text{SOD}}$ is that in the presence of SOD, taken at the concentration at which R_{MAX} attains the ultimate value (maximum when SOD stimulates the oxidation and minimum when SOD inhibits the oxidation). In the absence of SOD the oxidation of non-substituted 1,4-hydroquinone QH₂ 1 occurs very slowly, as has been earlier reported.^{3,7} The presence of one, two, or three alkyl substituents (QH₂ 2, 3, 5–8 and 11) results in a moderate

increase in R_{MAX} . QH₂ 4, with a bulky substituent, oxidizes 4–5-fold slower than its non-hindered analogs QH₂ 2 and QH₂ 3 (Table 1). The addition of SOD causes a pronounced increase in R_{MAX} , being also accompanied by alteration of the shape of [O₂] traces from the (-) to S-type for non-substituted 1,4-hydroquinone QH₂ 1 and monoalkyl-substituted hydroquinones, and by slight alteration for dialkyl-substituted hydroquinones (Fig. 2). As seen from Fig. 2, the increase in R_{MAX} may go together with the reduction of the rate of oxygen consumption at the early stage of the process. By contrast to oxidation without SOD, R_{MAX} during oxidation in the presence of SOD decreases dramatically with the increase in the number of alkyl-substituents (Table 1).

1,4-Hydroquinones QH₂ 9, QH₂ 10, and QH₂ 12, possessing strong electron-donating groups, display rather high oxidizability even in the absence of SOD. Adding SOD stimulates moderately the oxidation of QH₂ 9 and QH₂ 12, but markedly inhibits that of QH₂ 10 (Table 1). All the tested 1,4-dihydroxynaphthalenes QH₂ 13, QH₂ 14, and QH₂ 15 as well as 9,10-dihydroxyphenanthrene QH₂ 16 show generally much higher susceptibility to oxidation than substituted 1,4-hydroquinones. SOD displays a moderate influence on the rate of oxidation of the compounds belonging to this group (Table 1).

As mentioned in the Introduction section, the comparison between the kinetic observations obtained in this work and those reported in the literature is rather complicated. However, some qualitative coincidences can be noted. In agreement with our data, ref. 3 has reported that the oxidizability of methyl-substituted 1,4-hydroquinones increases with the increase in the number of methyl groups from zero to three and the rate of the autoxidation of these QH₂ is stimulated by SOD. The general tendency of SOD to inhibit or stimulate QH₂ autoxidation, which has been reported in the literature^{1,2,3,9} and observed in this work, is not generally in conflict. In both cases, the boundary, where the inhibition gives way to stimulation, is located nearby $E(\text{O}_2/\text{O}_2^{\cdot-}) = -155 \text{ mV}$. Meanwhile, it is not always possible to write unambiguously about the stimulating or inhibiting effect of SOD; sometimes the increase in R_{MAX} with addition of SOD is accompanied by visible inhibition of the oxidation at the early stage, as exemplified by Fig. 2A for QH₂ 2. Similar behavior was also observed for non-substituted 1,4-dihydroxynaphthalene QH₂ 13, both in our work (not shown) and in ref. 12.

Factors affecting the kinetics of hydroquinone oxidation

As it has been well documented in this (Table 1) and previous works,^{1,3,9} the addition of SOD may cause both stimulatory and inhibitory effects on QH₂ oxidation. No matter what the character of the SOD effect is, this tends to the saturation with [SOD] (Fig. 3). The region of [SOD] where a significant change in R_{MAX} is observed varies over a wide range depending on QH₂ structure. For example, the SOD concentration which provides 50% of the extreme effect, $[\text{SOD}]_{50}$, has been found to be of ca. 300 U ml^{-1} for the oxidation of 100 μM 1 (estimated on the basis of the data reported in ref. 7), 85 \pm 10 U ml^{-1} for 100 μM 2, 2.8 \pm 0.3 U ml^{-1} for 100 μM 5, 1.5 \pm 0.2 U ml^{-1} for 50 μM 10, and 0.25 \pm 0.05 U ml^{-1} for 50 μM 14. Among other things, we can notice that $[\text{SOD}]_{50}$ decreases dramatically with the increase in number of methyl substituents in 1,4-hydroquinone. With 1,4-hydroquinone QH₂ 1, as well as with mono- and dialkyl-substituted 1,4-hydroquinones, the increase of [SOD] results in progressive displacement of IP in the direction of its maximum position (corresponding to 50% conversion) as exemplified by Fig. 2.

With all the studied hydroquinones, R_{MAX} increases with pH (not shown), which correlates with a similar effect for the constant of equilibrium (1) reported in ref. 22. Depending on QH₂ structure and SOD added, the pH effect on R_{MAX} varies in the vicinity of pH 7.4 within the range from 2.7 to 4.5% per 0.01

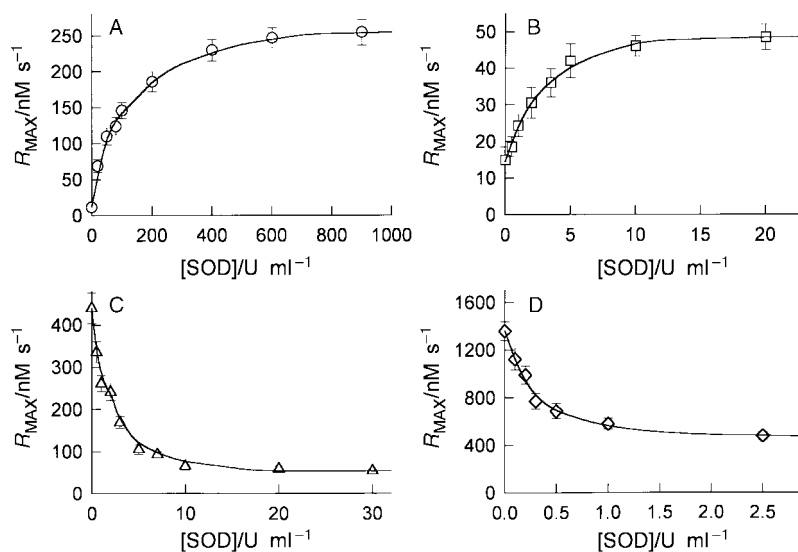


Fig. 3 Effect of SOD on R_{MAX} during the oxidation of QH_2 : A, 100 μM **2**; B, 100 μM **5**; C, 50 μM **10**; D, 50 μM QH_2 **14**. Conditions are: phosphate buffer, pH 7.4, 37 °C.

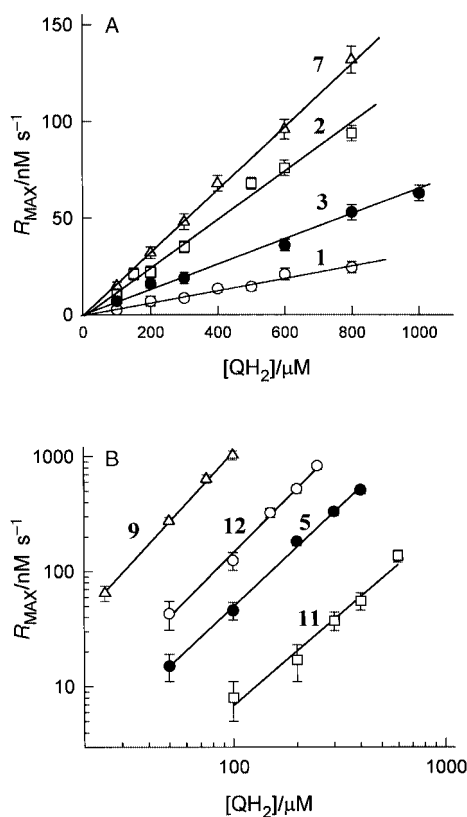


Fig. 4 Concentration effects on R_{MAX} during the oxidation of various QH_2 in the absence of SOD (A) and at optimal SOD concentration for different QH_2 (B) (see text and Fig. 3). Conditions are: 50 mM phosphate buffer, pH 7.4, 37 °C. Labels on plots are QH_2 compound numbers.

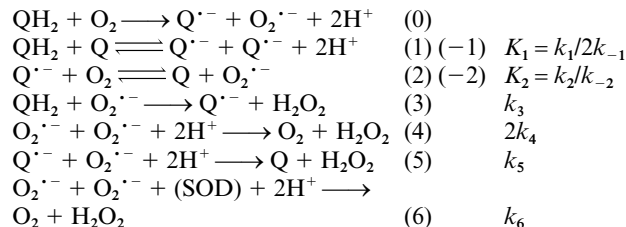
pH unit. Elevation of temperature stimulates the oxidation; R_{MAX} typically doubles per 10 °C increase (not shown).

Adding Q, a principle product of QH_2 autoxidation, at a concentration that is only a small fraction of the initial concentration of QH_2 , produces typically a moderate, if any, stimulatory effect on the rate of oxidation. If we deal with $[\text{O}_2]$ traces of the (S)-type, the addition of a low concentration of Q reduces the period of time, t_{IP} , required to reach IP (shortening lag period); for example, addition of 5 μM Q **2** to 100 μM QH_2 **2** results in the decrease of t_{IP} from 9 to 5 min. By contrast, when QH_2 oxidation displays $[\text{O}_2]$ traces of the (-)-type, the addition of Q does not cause any change in R_{MAX} (not shown).

Most typically, R_{MAX} increases directly with $[\text{QH}_2]$ when QH_2 is oxidized in the absence of SOD (Fig. 4A). When the oxidation occurs with added SOD, R_{MAX} has been found to be nearly proportional to $[\text{QH}_2]^2$ (Fig. 4B).

Kinetic computer simulation

Kinetic scheme. The autoxidation of QH_2 may be described by Scheme 1. As Scheme 1 suggests, QH_2 autoxidation is a



Scheme 1

chain (cyclic) process with semiquinone ($\text{Q}^{\cdot-}$) and superoxide ($\text{O}_2^{\cdot-}$) as chain propagating species. Reaction (0), as it has been indicated in the Introduction section, is spin forbidden and its role under physiological conditions can be neglected. Autoxidation is really initiated by reaction (1). At least traces of Q are necessary to start the process; this seems to be always realistic since small amounts of Q are present even in thoroughly purified QH_2 samples. QH_2 and oxygen are consumed *via* reactions (1) and (2), respectively. The former is also consumed *via* reaction (3) in the absence of SOD. Q is produced in reaction (2) and probably in reaction (5). The addition of SOD results in the decrease in the steady-state concentration of $\text{O}_2^{\cdot-}$ and hence the decrease in the contribution of reactions (-2), (3) and (5). As for reaction (4), it is too slow at neutral pH²³ to play any significant role even in the absence of SOD. The scheme predicts the 1:1:1 stoichiometry for the consumption of QH_2 and oxygen, and accumulation of Q and H_2O_2 . The latter may be considered as a basis for the various methods of monitoring QH_2 oxidation.

Rate constants for individual stages. Before the results of the simulation are presented, we should consider the availability of the information on rate constants for the individual stages (in $\text{M}^{-1} \text{s}^{-1}$) included in Scheme 1. The rate constants for the majority of these reactions are pH-dependent, as they occur both with protonated and deprotonated forms, for example with QH_2 , QH^- and Q^{2-} for hydroquinones. This is one reason why rate constants used in this work are only effective values;

Table 2 Thermodynamic and kinetic parameters determining the kinetics of hydroquinone oxidation

QH ₂ ^a	$E(Q/Q^{\cdot-})/$ mV ^b	$E(Q^{\cdot-}/QH_2)/$ mV ^b	$\Delta E_1/$ mV ^c	$k_1/$ M ⁻¹ s ⁻¹ ^d
1	+78	+448 ^e	-370	1300
2	+23	+414 ^e	-391	450
3	nd	nd	-395	290
4	-32 ^f	+453 ^e	-485	3
5	-80	+363 ^e	-443	50
6	-74	+430	-504 ^g	6.3 ^h
7	-67	+420	-487 ^g	9.3 ⁱ
8	nd	nd	-428	30
9	-150	-187 ^e	-337	800
10	-232 ^j	<282 ^k	nd	nd
11	-165	+385	-550 ^g	1.1 ^l
12	-110	+290	-399	140
13	-140	+238 ^e	-380	1400
14	-203	+190	-393 ^g	520 ^m
15	-36	nd	nd	nd
16	-124	+178 ⁿ	-302 ^g	7800 ^o

nd = Not determined. ^a Structures of QH₂ are given in the text. ^b At 25 °C and pH 7.0, taken from refs. 3 and 33 unless otherwise indicated. ^c At 25 °C and pH 7.0, taken from ref. 22 unless otherwise indicated. ^d At 37 °C and pH 7.40; taken from ref. 22 unless otherwise indicated. ^e Taken from ref. 22. ^f Taken from ref. 34. ^g Calculated from E_1 and E_2 . ^h Calculated from ΔE_1 in combination with $2k_{-1} = 1.55 \times 10^8 \text{ M}^{-1} \text{ s}^{-1}$.²⁸ ⁱ Calculated from ΔE_1 in combination with $2k_{-1} = 1.20 \times 10^8 \text{ M}^{-1} \text{ s}^{-1}$.²⁸ ^j Assumed to be equal to that reported for the quinone produced from TOPA.³⁵ ^k Taken from ref. 5. ^l Calculated from ΔE_1 in combination with $2k_{-1} = 1.55 \times 10^8 \text{ M}^{-1} \text{ s}^{-1}$.²⁸ ^m Calculated from ΔE_1 in combination with $2k_{-1} = 2 \times 10^8 \text{ M}^{-1} \text{ s}^{-1}$.³ ⁿ Taken from ref. 11. ^o Calculated from ΔE_1 assuming that $2k_{-1}$ is as much as $1 \times 10^8 \text{ M}^{-1} \text{ s}^{-1}$.

they are given at physiological pH 7.4 throughout the text. Mid-point, one-electron reduction potentials used in this work are also pH-dependent; they are commonly given at pH 7.0. The values of $2k_4$ (2×10^{23}) and k_6 (2×10^9)—the average value for numerous determinations²⁴) are evidently independent of QH₂ structure. The constant for equilibrium (2), $K_2 = k_2/k_{-2}$, is definitively determined by the position of one-electron reduction potential $E(Q/Q^{\cdot-})$ relative to $E(O_2/O_2^{\cdot-}) = -155 \text{ mV}$; ^{25,26} in particular, $K_2 = 1$ if $E(Q/Q^{\cdot-})$ is as much as -155 mV . The rate constants k_2 and k_{-2} at neutral pH are related by the expression $2k_2k_{-2} \approx 1 \times 10^{14} - 1 \times 10^{15}$, as may be estimated on the basis of data reported in refs. 3, 25–27. For the majority of $Q^{\cdot-}$, $2k_{-1}$ has been found to be nearly 1×10^8 ; ^{1,28} $2k_{-1}$ has been reported to be significantly lower only for a few $Q^{\cdot-}$ such as aziridinyl-²⁹ and methoxy-substituted $Q^{\cdot-}$.²⁸ The information on k_3 in the literature is rather poor and conflicting; a typical value of k_3 is 1×10^5 .^{30–32} From general considerations, k_3 is expected to increase when the reduction potential $E(Q^{\cdot-}/QH_2)$ decreases. A value of k_5 for the reaction of cross-dismutation (5) is not known. Fortunately, it is not so important for simulations since in most cases the variations in k_3 and k_5 result in only moderate, if any, effects on the kinetics. In the further simulations k_5 is assumed to be of the order 1×10^8 .

As will be shown below, QH₂ oxidation in the presence of a high enough concentration of SOD, typical of real biological environment, occurs in the mode where the rate of the process is almost definitively determined by the rate of reaction (1). Until recently, the information on k_1 under physiological conditions (at neutral pH) has been very poor. Our recent work,²² where k_1 was determined for several Q/QH₂ couples, has partly eliminated this gap. The known values of k_1 are listed in Table 2. The most general way to determine k_1 is based on eqn. (7). K_1 can be

$$K_1 = k_1/2k_{-1} \quad (7)$$

determined by EPR from the steady-state concentration of $Q^{\cdot-}$ in the mixture of Q and QH₂.^{22,34,36} In turn, $2k_{-1}$ can be directly determined from the kinetics of $Q^{\cdot-}$ decay by the pulse radioly-

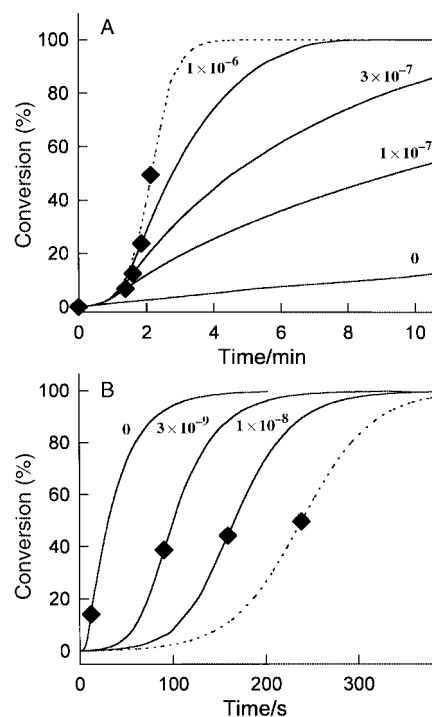


Fig. 5 Effect of SOD on the kinetics of QH₂ autoxidation as simulated on the basis of Scheme 1 with kinetic parameters reported for QH₂ 2 (A) and QH₂ 14 (B). Dotted lines show kinetic curves at [SOD] → ∞. Figures on traces indicate SOD concentration given in M. Rate constants are given in M⁻¹ s⁻¹. Kinetic parameters taken in the simulations were for A: [QH₂]₀ = 100 μM; [Q]₀ = 0.3 μM; [O₂]₀ = 200 μM; $k_1 = 450$,²² $2k_{-1} = 1.35 \times 10^8$,²⁸ $k_2 = 1.1 \times 10^6$,²⁷ $k_{-2} = 7.6 \times 10^8$,²⁷ $k_3 = 2 \times 10^4$ (assumed); $2k_4 = 2 \times 10^5$,²³ $k_5 = 2 \times 10^8$ (assumed); $k_6 = 2 \times 10^9$.²⁴ For B: [QH₂]₀ = 50 μM; [Q]₀ = 0.1 μM; [O₂]₀ = 200 μM; $k_1 = 520$ (see Table 1); $2k_{-1} = 2 \times 10^8$,³ $k_2 = 2.4 \times 10^8$,²⁷ $k_{-2} = 3.8 \times 10^7$,²⁷ $k_3 = 1 \times 10^5$ (assumed); $k_5 = 2 \times 10^8$ (assumed); $2k_4$ and k_6 are the same as in the case of A.

sis technique.²² If K_1 has not been measured directly, it may be estimated from the difference of one-electron reduction potentials, eqn. (8) by using the Nernst equation (9), where ΔE_1 is

$$\Delta E_1 = E(Q/Q^{\cdot-}) - E(Q^{\cdot-}/QH_2) \quad (8)$$

$$\ln K_1 = a\Delta E_1 \quad (9)$$

given in mV and coefficient a depends on temperature ($a = 0.0389 \text{ mV}^{-1}$ at 25 °C and 0.0374 mV^{-1} at 37 °C).

The comparison between the simulated and experimental [O₂] traces. Prior to the study of fine kinetic details of QH₂ autoxidation, we should make sure that the procedure of simulation based on Scheme 1 is capable of reproducing the kinetic curves observed experimentally. This is demonstrated in Fig. 5. The plots presented in Fig. 5A were simulated with the kinetic parameters reported in the literature for QH₂ 2. The comparison of [O₂] traces presented in Fig. 5A with those in Fig. 2A suggests that the simulation reasonably reproduces the main features of experimental traces—going from a trace of (–)-type to traces of S-type when SOD is added; the increase in R_{MAX} with [SOD]; a progressive shifting of IP in the direction of higher conversion as [SOD] increases. Moreover, the simulated quantitative characteristics of the process are also found to be in reasonable agreement with those determined experimentally. Among other things, the simulated values of R_{MAX} in the absence of SOD and at [SOD] → ∞, 17.4 and 1120 nM s⁻¹, respectively (Fig. 5A), are not much different from experimental values, 12.5 nM s⁻¹ (no SOD) and 250 nM s⁻¹ (900 U ml⁻¹ SOD) (Fig. 2A). The plots presented in Fig. 5B were simulated with kinetic parameters reported for QH₂ 14. When the simulated plots (Fig. 5B) are compared with experimental ones

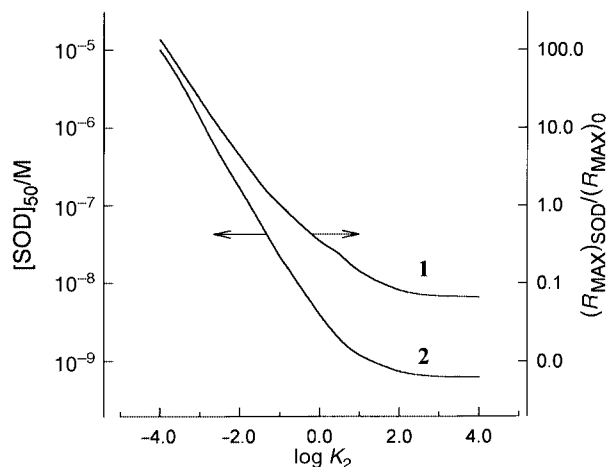


Fig. 6 The influence of K_2 on $(R_{\text{MAX}})_{\text{SOD}}/(R_{\text{MAX}})_0$ (plot 1) and $[\text{SOD}]_{50}$ (plot 2) during the oxidation of $100 \mu\text{M}$ QH_2 containing $1 \mu\text{M}$ Q as simulated on the basis of Scheme 1. Parameters are given in $\text{M}^{-1} \text{s}^{-1}$; the references are given in the text): $k_1 = 300$; $2k_{-1} = 1 \times 10^8$; $k_2 k_{-2} = 1 \times 10^{14}$; $k_3 = 1 \times 10^5$; $2k_4 = 2 \times 10^5$; $k_5 = 1 \times 10^8$; $k_6 = 2 \times 10^9$; $[\text{O}_2] = 200 \mu\text{M}$.

(Fig. 2B), we can highlight again their reasonable similarity. In all cases, adding SOD results in slowing down the oxidation (decrease in R_{MAX} and shifting IP to longer times). Significantly, the simulation predicts that the effective SOD concentrations in the case of QH_2 14 are two orders of magnitude less than that of QH_2 2, which is in accordance with the experiment (Fig. 2 and 3). As with QH_2 14, a reasonable agreement between the simulated and experimental values of R_{MAX} is observed: 1130 nM s^{-1} at $[\text{SOD}] = 0$ and 325 nM s^{-1} at $[\text{SOD}] \rightarrow \infty$ (simulation, Fig. 5B); 1360 nM s^{-1} at $[\text{SOD}] = 0$ and 440 nM s^{-1} at 10 U ml^{-1} SOD (experiment, Fig. 2B). In conclusion, the simulations on the basis of Scheme 1 using the reported rate constants for individual stages are able to predict, at least semi-quantitatively, the kinetics of QH_2 oxidation and influence of SOD on the process.

Now we can enter into a more detailed consideration of the main factors affecting the kinetics of QH_2 oxidation.

Effect of SOD concentration. As is evident from Scheme 1, purging the system of $\text{O}_2 \cdot^-$ by SOD results in the shift of the equilibrium (2) to the right, as well as in inhibiting reactions (3) and (5). The net effect of SOD addition on the oxidation may be either stimulatory or inhibitory. The value of K_2 is a key factor, which determines the character of the SOD effect. To a first approximation, the boundary value of K_2 , where the stimulatory action of SOD becomes inhibitory, is expected to be near 1. In turn, K_2 is uniquely determined by the one-electron reduction potential $E(\text{Q}/\text{Q}^{\cdot-})$, K_2 being equal to 1 when $E(\text{Q}/\text{Q}^{\cdot-}) = E(\text{O}_2/\text{O}_2^{\cdot-}) = -155 \text{ mV}$.³³ As may be inferred from comprising the data presented in Tables 1 and 2 and has been repeatedly suggested in the literature,^{1,3} the alteration of the character of the SOD effect from stimulatory to inhibitory does occur near $E(\text{Q}/\text{Q}^{\cdot-}) = -155 \text{ mV}$. The $(R_{\text{MAX}})_{\text{SOD}}/(R_{\text{MAX}})_0$ ratio, which quantitatively characterizes the SOD effect, increases progressively with $E(\text{Q}/\text{Q}^{\cdot-})$ (Tables 1 and 2). The additional information may be obtained using kinetic simulation (Fig. 6). The simulation predicts the following effects:

(i) The boundary value of K_2 , where the SOD effect changes its sign from positive to negative, is shifted from 1 to nearly 0.1. This is associated with the fact that adding SOD not only shifts equilibrium (2) to the right, but this is also accompanied by inhibition of reactions (3) and (5).

(ii) The accelerating effect of SOD in the region of $K_2 < 0.1$ is generally more pronounced than the inhibitory effect, which is observed at $K_2 > 0.1$ (see also Fig. 3). In the region of $K_2 < 0.1$,

Table 3 The effect of $[\text{O}_2]$ on R_{MAX} during the oxidation of $100 \mu\text{M}$ QH_2 in the presence of $1 \times 10^{-6} \text{ M}$ SOD at various values of K_2 as simulated on the basis of Scheme 1. All the other kinetic parameters are as given in the legend to Fig. 6

$[\text{O}_2]/\mu\text{M}$	$R_{\text{MAX}}/\text{nM s}^{-1}$		
	$K_2 = 0.01$	$K_2 = 1$	$K_2 = 100$
200	744	766	767
20	347	759	767
2	48.4	484	761
0.2	5.03	75.9	506

the higher $(R_{\text{MAX}})_{\text{SOD}}/(R_{\text{MAX}})_0$, the lower K_2 (Fig. 6). This is in reasonable agreement with the experimental data (Tables 1 and 2). When K_2 exceeds 0.1, the opposite tendency is observed— $(R_{\text{MAX}})_{\text{SOD}}/(R_{\text{MAX}})_0$ decreases with increasing K_2 .

(iii) $[\text{SOD}]_{50}$ decreases dramatically with K_2 , but the effect becomes less pronounced as K_2 increases (Fig. 6, plot 2). When $K_2 > 10^3$, $[\text{SOD}]_{50}$ ceases to depend on K_2 and tends to the limit of *ca.* $5 \times 10^{-10} \text{ M}$ (about 0.04 U ml^{-1}). The latter is in reasonable agreement with experimentally determined values of $[\text{SOD}]_{50}$ for QH_2 14 (0.25 U ml^{-1} , Fig. 3D) and 0.02 U ml^{-1} reported in ref. 37 for 2,3-dimethyl-1,4-dihydroxynaphthalene.

(iv) The positions of the plots of $(R_{\text{MAX}})_{\text{SOD}}/(R_{\text{MAX}})_0$ and $[\text{SOD}]_{50}$ against K_2 presented in Fig. 6 are not universal; they depend somewhat on several parameters, with k_1 and QH_2 concentration giving the most significant effect. For instance, when k_1 alters from $300 \text{ M}^{-1} \text{ s}^{-1}$ to $3000 \text{ M}^{-1} \text{ s}^{-1}$, $(R_{\text{MAX}})_{\text{SOD}}/(R_{\text{MAX}})_0$ increases from 0.0675 to 0.230 (at $K_2 = 100$); when $[\text{QH}_2]$ alters from $100 \mu\text{M}$ to $10 \mu\text{M}$, $(R_{\text{MAX}})_{\text{SOD}}/(R_{\text{MAX}})_0$ changes from 137 to 21.4 and $[\text{SOD}]_{50}$ changes from $1.0 \times 10^{-5} \text{ M}$ to $1.3 \times 10^{-7} \text{ M}$ (at $K_2 = 1 \times 10^{-4}$). However, a variation of kinetic parameters within reasonable limits does not change the general kinetic picture.

(v) Starting with the hydroquinones for which K_2 exceeds *ca.* 0.001 (this nearly corresponds to $E_1(\text{Q}/\text{Q}^{\cdot-}) = -20 \text{ mV}$), $[\text{SOD}]_{50}$ is predicted to be less than $5 \times 10^{-7} \text{ M}$, a value lower than the common concentration of SOD in tissues *in vivo* (10^{-5} – 10^{-6} M ^{38,39}). Among other things, this means that the kinetic information on the autoxidation of the majority of QH_2 has a relevance to biological problems only when the process is studied in the presence of SOD.

The simulations predict that when QH_2 autoxidation occurs in the presence of a high enough concentration of SOD ($[\text{SOD}] \gg [\text{SOD}]_{50}$), the position of the IP is always located near 50% conversion and R_{MAX} is almost definitively determined by the rate of reaction (1), resulting in eqn. (10), and only moderately

$$R_{\text{MAX}} = 0.25k_1 \times [\text{QH}_2]_0^2 \quad (10)$$

depends on any other factor. By way of illustration, we consider how R_{MAX} depends on $[\text{O}_2]$ (Table 3). It is seen that R_{MAX} only moderately decreases with $[\text{O}_2]$ in going $[\text{O}_2]$ from $200 \mu\text{M}$, typical of kinetic laboratory test, to $20 \mu\text{M}$, typical of tissues *in vivo*. This holds true even at $0.2 \mu\text{M}$ O_2 (which corresponds to a very severe hypoxia) provided that K_2 exceeds 100 ($E_1(\text{Q}/\text{Q}^{\cdot-}) < -270 \text{ mV}$). This observation permits almost direct extrapolation of the kinetic information on QH_2 oxidation (in the presence of SOD only!) obtained *via* a routine laboratory test to the *in vivo* conditions.

Fig. 7 shows how R_{MAX} depends on QH_2 concentration at various modes of the process. The relationship between R_{MAX} and $[\text{QH}_2]$ may be given by the general equation (11), where

$$R_{\text{MAX}} \sim [\text{QH}_2]^n \quad (11)$$

n varies from 0.5 to 2 depending on the kinetic situation. With-

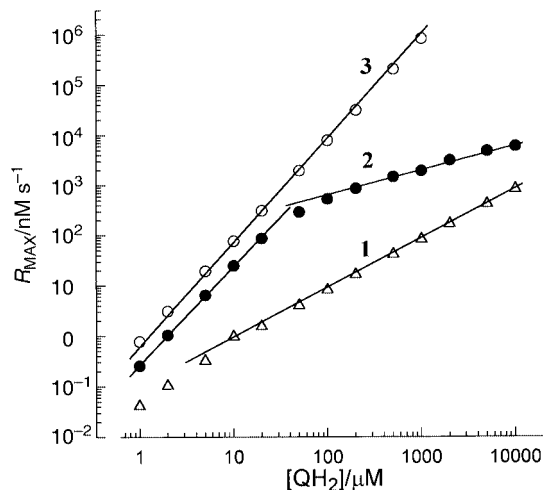


Fig. 7 $[\text{QH}_2]$ plots of R_{MAX} during the oxidation of QH_2 simulated on the basis of Scheme 1 under various conditions (rate constants are given in $\text{M}^{-1} \text{s}^{-1}$): Plot 1, $k_1 = 1000$; $K_2 = 1 \times 10^{-4}$; $[\text{O}_2] = 200 \mu\text{M}$; $[\text{SOD}] = 0$. Plot 2, the same as plot 1 with the exception that $[\text{SOD}] = 1 \times 10^{-3} \text{M}$. Plot 3, the same as plot 1 with the exception that $k_1 = 3000$; $K_2 = 1$ and $[\text{SOD}] = 1 \times 10^{-6} \text{M}$. All the other parameters are as indicated in the legend to Fig. 6.

out SOD, R_{MAX} increases basically directly with $[\text{QH}_2]$ (Fig. 7, plot 1) as has been observed experimentally (Fig. 4A). When SOD is added and K_2 is not too low, R_{MAX} increases nearly proportionally to $[\text{QH}_2]^2$ over a wide range of $[\text{QH}_2]$ in accordance with the observations presented in Fig. 4B (Fig. 7, plot 3). When SOD is added, but K_2 is very low, R_{MAX} is proportional to $[\text{QH}_2]^2$ at low concentrations of QH_2 and to $[\text{QH}_2]^{0.5}$ when $[\text{QH}_2]$ is high enough (Fig. 7, plot 2). A plot of this kind was reported in ref. 7 for the oxidation of non-substituted 1,4-hydroquinone QH_2 **1** ($K_2 = 5 \times 10^{-527}$) in the presence of high concentrations of SOD. Each index of power in eqn. (11) (0.5, 1 or 2) corresponds to a certain path of chain termination: $n = 0.5$ means that the chain termination occurs mainly by reaction (–1); when $n = 1$, chain termination occurs by cross-dismutation (reaction (5)); $n = 2$ corresponds to the situation when reaction (6) is the main way for the decay of $\text{O}_2^{\cdot-}$ and $\text{Q}^{\cdot-}$ does not participate in termination. The latter case seems to be of most biological significance. Additionally, this mode can be described by a very simple kinetic scheme, which includes only three reactions, (1), (2) and (6).

The correlation between R_{MAX} and rate constants for comproportionation of hydroquinone and quinone

It has been demonstrated that the maximum rate of the process is definitively determined by the rate of comproportionation between Q and QH_2 (reaction (1)) if QH_2 oxidation occurs at a high enough concentration of SOD. Moreover, this mode of the process is suggested to be the most realistic in biological systems under *in vivo* conditions. Fig. 8 depicts the correlation between R_{MAX} determined at the optimal concentration of SOD (when SOD effect is saturated, see Fig. 3) and k_1 . As we might expect, $\log R_{\text{MAX}}$ shows a reasonably linear correlation with $\log k_1$ ($r^2 = 0.935$) without considering data for QH_2 **6**, QH_2 **7** and QH_2 **11**. The slope of the plot was found to be as much as 1.02 ± 0.04 ; this means that R_{MAX} is proportional to the rate of reaction (1), with other factors being almost negligible. The most probable reason why QH_2 **6**, QH_2 **7** and QH_2 **11** drop out from the correlation is that values of k_1 for these compounds have not been previously determined, but estimated from the difference of one-electron reduction potentials $\Delta E_1 = E(\text{Q}/\text{Q}^{\cdot-}) - E(\text{Q}^{\cdot-}/\text{QH}_2)$. There are grounds to suspect that the values of $E(\text{Q}^{\cdot-}/\text{QH}_2)$ for QH_2 **6**, QH_2 **7** and QH_2 **11**, reported in the single work⁴⁰ and not confirmed by other publications, are somewhat over-

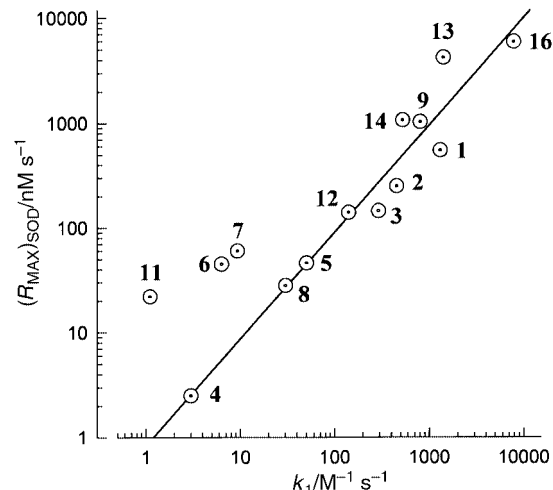


Fig. 8 The correlation between R_{MAX} determined when $100 \mu\text{M}$ QH_2 is oxidized in 0.05M phosphate buffer, pH 7.40, at 37°C in the presence of the optimal concentration of SOD (see text for more detail) and the rate constant for reaction (1). The values of R_{MAX} and k_1 were taken from Table 1 and Table 2, respectively. Labels at symbols represent QH_2 compound numbers.

estimated.[†] This may result in underestimating k_1 calculated in this work by using eqns. (7)–(9).

The above correlation can be used to predict the oxidizability of other QH_2 based on their reduction potentials. For example, elevated oxidizability of several QH_2 ^{1,2} combines with elevated values of ΔE_1 . 1,4,5,8-Tetrahydroxynaphthalene ($E(\text{Q}/\text{Q}^{\cdot-}) = -110 \text{mV}$,³³ $E(\text{Q}^{\cdot-}/\text{QH}_2) = -15 \text{mV}$,⁴¹ and hence $\Delta E_1 = -95 \text{mV}$), 2,3-dimethoxy-1,4-dihydroxynaphthalene ($E(\text{Q}/\text{Q}^{\cdot-}) = -240 \text{mV}$,³ $E(\text{Q}^{\cdot-}/\text{QH}_2) = -90 \text{mV}$,³ and hence $\Delta E_1 = -130 \text{mV}$), and adriamycin ($E(\text{Q}/\text{Q}^{\cdot-}) = -341 \text{mV}$,³ $E(\text{Q}^{\cdot-}/\text{QH}_2) = -272 \text{mV}$,⁴¹ and hence $\Delta E_1 = +70 \text{mV}$) are some such examples. In turn, the correlation under consideration may be used to estimate one-electron reduction potentials from the rate of hydroquinone autoxidation determined in the presence of a high enough concentration of SOD. This approach is likely to be applicable to the oxidation of substrates other than QH_2 , for instance ascorbate.²²

Conclusion

QH_2 autoxidation is a chain autocatalytic process, with Q being a catalyst. When $[\text{SOD}]$ is high enough (at physiological level), the autoxidation can be described by a very simple kinetic scheme including only three reactions, (1), (2), and (6). Under these conditions, the rate of the process increases with conversion and peaks at about 50% conversion. The maximal rate of autoxidation is definitively determined by the rate of compro-

[†] As has been shown in our previous work,²² two one-electron reduction potentials, $E(\text{Q}^{\cdot-}/\text{QH}_2)$ and $E(\text{Q}/\text{Q}^{\cdot-})$, show excellent linear correlation between each other, provided that both potentials have been measured in the same organic solvent. It may be suggested that this situation holds true in aqueous solution if we deal with a relatively narrow group of compounds with non-polar substituents. The value of $E(\text{Q}/\text{Q}^{\cdot-})$ for three isomeric dimethylbenzo-1,4-quinones, QH_2 **5**, QH_2 **6** and QH_2 **7**, are very close to each other (Table 2). It could be expected that $E(\text{Q}^{\cdot-}/\text{QH}_2)$ for QH_2 **5**, QH_2 **6** and QH_2 **7** would have similar values. Contrary to the expectations, $E(\text{Q}^{\cdot-}/\text{QH}_2)$ for QH_2 **6** and QH_2 **7** presented in Table 2 and used in the correlation (Fig. 8), exceed that of QH_2 **5** by 55–60 mV. $E(\text{Q}/\text{Q}^{\cdot-})$ for trimethyl-substituted QH_2 **11** has been reported to be -165mV , *i.e.* 85 mV more negative than that for QH_2 **5** (Table 2). This suggests that $E(\text{Q}^{\cdot-}/\text{QH}_2)$ for QH_2 **11** is significantly less than that for QH_2 **5**, contrary to data given in Table 2. It has been estimated that decreasing $E(\text{Q}^{\cdot-}/\text{QH}_2)$ for QH_2 **6** and QH_2 **7** by about 40 mV and for QH_2 **11** by 70 mV relative to the figures presented in Table 2 would be enough to fit the data for QH_2 **6**, QH_2 **7** and QH_2 **11** into the linear correlation given in Fig. 8. The latter seems to be quite realistic.

portionation of QH₂ with the corresponding Q (reaction (1)). To a first approximation, the rate constant for reaction (1) is determined by the difference between two reduction potentials $\Delta E_1 = E(Q/Q^{\cdot-}) - E(Q^{\cdot-}/QH_2)$. Within a realistic region of QH₂ concentrations, the rate of oxidation in the presence of SOD is proportional to the square of QH₂ concentration. Other factors, including oxygen concentration, reactivity of Q^{•-} and reactivity of QH₂ towards O₂^{•-}, have a very moderate, if any, effect. The addition of SOD may either stimulate or inhibit the autoxidation. Both the sign of SOD effect (stimulation or inhibition) and its value ($R_{MAX}SOD/R_{MAX}0$) are basically determined by the reduction potential $E_1(Q/Q^{\cdot-})$. In contrast to the oxidation of QH₂ in the presence of SOD, the kinetics of this process in the absence of SOD are a complex function of many parameters. However, it should be noticed that this mode of QH₂ oxidation in fact bears no relation to the biological situation. The kinetics of QH₂ autoxidation under physiological conditions (in the presence of SOD) may be predicted provided that $E(Q/Q^{\cdot-})$ and k_1 (or at least $E(Q^{\cdot-}/QH_2)$) are known. Unfortunately, for many QH₂(Q) of biological significance k_1 and $E(Q^{\cdot-}/QH_2)$ are still unknown. This emphasizes the need for determination of the above parameters in further studies.

Acknowledgements

The present work was partly supported by grant 96-03-00103 from the Russian Foundation for Fundamental Researches. We thank A. Kryuchkov and L. Pisarenko for the synthesis and purification of several hydroquinones.

References

- 1 A. Brunmark and E. Cadenas, *Free Radical Biol. Med.*, 1989, **7**, 435.
- 2 A. Brunmark, in *Free Radicals in the Environment, Medicine and Toxicology*, ed. H. Nohl, H. Esterbauer and C. Rice-Evans, Richeheu Press, London, 1994, p. 119.
- 3 P. J. O'Brien, *Chem. Biol. Interact.*, 1991, **80**, 1.
- 4 S. P. Mayalarp, R. H. J. Hargreaves, J. Butler, C. C. O'Hare and J. A. Hartley, *J. Med. Chem.*, 1996, **39**, 531.
- 5 V. A. Roginsky, T. K. Barsukova, G. Bruchelt and H. B. Stegmann, *Z. Naturforsch., Teil C*, 1997, **52**, 380.
- 6 R. Jarabak and J. Jarabak, *Arch. Biochem. Biophys.*, 1995, **318**, 418.
- 7 P. Eyer, *Chem. Biol. Interact.*, 1991, **80**, 159.
- 8 A. Brunmark and E. Cadenas, *Chem. Biol. Interact.*, 1988, **68**, 273.
- 9 B. Bandy, J. Moon and A. J. Davison, *Free Radical Biol. Med.*, 1990, **9**, 143.
- 10 J. Butler, V. J. Spanswick and J. Cummings, *Free Radical Res.*, 1996, **25**, 141.

- 11 R. Jarabak, R. G. Harvey and J. Jarabak, *Arch. Biochem. Biophys.*, 1997, **339**, 92.
- 12 T. Ishii and I. Fridovich, *Free Radical Biol. Med.*, 1990, **8**, 21.
- 13 E. Cadenas, D. Mira, A. Brunmark, C. Lind, J. Segura-Aguilar and L. Ernsster, *Free Radical Biol. Med.* 1988, **5**, 71.
- 14 R. Munday, *Free Radical Biol. Med.*, 1997, **22**, 689.
- 15 L. Zhang, B. Bandy and A. I. Davison, *Free Radical Biol. Med.*, 1996, **20**, 495.
- 16 G. D. Buffinton, K. Öllinger, A. Brunmark and E. Cadenas, *Biochem. J.*, 1989, **257**, 561.
- 17 D. G. Graham, S. M. Tiffany, W. R. Bell and W. F. Gutknecht, *Mol. Pharmacol.*, 1978, **14**, 644.
- 18 V. A. Roginsky and H. B. Stegmann, *Free Radical Biol. Med.*, 1994, **17**, 93.
- 19 V. A. Roginsky, T. K. Barsukova, G. Bruchelt and H. B. Stegmann, *Free Radical Res.*, 1998, **29**, 115.
- 20 V. A. Roginsky, G. Bruchelt and O. Bartuli, *Biochem. Pharmacol.*, 1998, **55**, 85.
- 21 V. A. Roginsky, T. K. Barsukova and H. B. Stegmann, *Chem. Biol. Interact.*, 1999, **121**, 177.
- 22 V. A. Roginsky, L. M. Pisarenko, W. Bors and C. Michel, *J. Chem. Soc., Perkin 2 Trans.*, 1999, 871.
- 23 B. H. J. Bielski, R. L. Cabelli, R. L. Arudi and A. B. Ross, *J. Phys. Chem. Ref. Data*, 1985, **14**, 1041.
- 24 I. B. Afanas'ev, *Superoxide Ion: Chemistry and Biological Implications*, vol. 2, CRC Press, Boca Raton, Florida, 1991.
- 25 P. Wardman, *Free Radical Res. Commun.*, 1990, **8**, 219.
- 26 D. Meisel, *Chem. Phys. Lett.*, 1975, **34**, 263.
- 27 Landolt-Börnstein, *Numerical Data and Functional Relationships in Science and Technology, New Series, Group II*, vol. 13e, Springer Verlag, Berlin, 1984.
- 28 V. A. Roginsky, L. M. Pisarenko, W. Bors, C. Michel and M. Saran, *J. Chem. Soc., Faraday Trans.*, 1998, **94**, 1835.
- 29 J. Butler, B. M. Hoey and J. S. Lea, *Biochim. Biophys. Acta*, 1987, **925**, 144.
- 30 S. Kitagawa, H. Fujisawa and H. Sakurai, *Chem. Pharm. Bull.*, 1992, **40**, 304.
- 31 D. J. Deeble, B. J. Parsons, G. O. Phillips, H.-P. Schuchmann and C. von Sonntag, *Int. J. Radiat. Biol.*, 1988, **54**, 179.
- 32 I. B. Afanas'ev, *Superoxide Ion: Chemistry and Biological Implications*, vol. 1, CRC Press, Boca Raton, Florida, 1989.
- 33 P. Wardman, *J. Phys. Chem. Ref. Data*, 1989, **18**, 1637.
- 34 J. K. Dohrman and B. Bergmann, *J. Phys. Chem.*, 1995, **99**, 1218.
- 35 K. Kano, T. Mori, B. Uno, M. Goto and T. Ikeda, *Biochim. Biophys. Acta*, 1993, **1157**, 324.
- 36 A. E. Alegria, M. Lopez and N. Guevara, *J. Chem. Soc., Faraday Trans.*, 1996, **92**, 4965.
- 37 R. Munday, *Free Radical Biol. Med.*, 1999, **26**, 1475.
- 38 S. K. Marklund, in *Oxygen Radicals in Chemistry and Biology*, eds. W. Bors, M. Saran and D. Tait, Walter de Gruyter & Co., Berlin & New York, 1984, p. 765.
- 39 R. Munday, *Redox Rep.*, 1997, **3**, 189.
- 40 Y. A. Ilan, G. Czapsky and D. Meisel, *Biochim. Biophys. Acta*, 1976, **430**, 209.
- 41 T. Mukherjee, *Radiat. Phys. Chem.*, 1987, **29**, 455.